Comparison of the Guarded-Heat-Flow and Transient-Plane-Source Methods for Carbon-Filled Nylon 6,6 Composites: Experiments and Modeling

Michael G. Miller, Jason M. Keith, Julia A. King, Rebecca A. Hauser, Angela M. Moran

Department of Chemical Engineering, Room 203, Chemical Sciences and Engineering Building, 1400 Townsend Drive, Michigan Technological University, Houghton, Michigan 49931-1295

Received 13 January 2005; accepted 5 June 2005
DOI 10.1002/app.22754
Published online 6 December 2005 in Wiley InterScience (www.interscience.wiley.com).

ABSTRACT: In this study, two different carbons (synthetic graphite particles and carbon fiber) were added to nylon 6,6, and the resulting composites were tested for thermal conductivity. The first goal of this work was to compare through-plane thermal conductivity results from the guarded-heat-flow method and the transient-plane-source method. The results showed that both test methods gave similar through-plane thermal conductivity results for composites containing 10–40 wt % synthetic graphite and for composites containing 5–40 wt % carbon fiber. The advantages of using the transient-plane-source method were that the in-plane thermal conductivity was also measured and the experimental time was shorter than that of the guarded-heat-flow method. The second goal of this work was to develop and use a detailed finite-element analysis to model heat transfer within a carbon-filled nylon 6,6 composite sample for the transient-plane-source method and compare these results to actual experimental results. The results showed that the finite-element model compared well with the actual experimental data. The finite-element model could be used in the future as a design tool to predict the dynamic thermal response of different composite materials for many applications. © 2005 Wiley Periodicals, Inc. J Appl Polym Sci 99: 2144–2151, 2006

Key words: fibers; modeling; nylon; thermal properties

INTRODUCTION

Most polymer resins are thermally insulating. Increasing the thermal conductivity of these resins opens large, new markets. The advantages of conductive resins, in comparison with metals (typically used), include improved corrosion resistance, lighter weight, and the ability to adapt the conductivity properties to suit the application needs. For example, a thermally conductive resin is ideally suited for heat-sink applications, such as lighting ballasts and transformer housings.

Typical thermal conductivity values for some common materials are 0.2–0.3 W/m K for polymers, 234 W/m K for aluminum, 400 W/m K for copper, and 600 W/m K for graphite. One approach to improving the thermal conductivity of a polymer is the addition of a conductive filler material, such as carbon or metal. Conductive resins with a thermal conductivity of approximately 1–30 W/m K can be used in heat-sink applications.[1]

A significant amount of work has been conducted in which the amounts of single conductive fillers have been varied in a composite material.[2–9] For example, ceramic fibers and particles (boron nitride, aluminum nitride, and aluminum oxide), metal fibers and particles (aluminum, steel, iron, copper, and silver), and nickel-coated glass fibers have been used.[1,3,10–12] Metallic fillers have several disadvantages, in comparison with carbon, which include higher density and greater susceptibility to oxidation. Various types of carbons are used as effective conductive fillers. For example, synthetic graphite particles and carbon fibers are often added to polymers to increase the composite thermal conductivity.[1,7,9,13–15]

In this project, researchers performed compounding runs followed by the injection molding of carbon-filled nylon 6,6 test specimens. Material characterization tests included thermal conductivity and optical microscopy to determine the aspect ratio and orientation angle of the conductive fillers. The two carbon fillers investigated were Thermocarb TC-300 specialty graphite from Conoco (recently purchased by Asbury Carbon, Asbury, NJ) and ThermalGraph DKD X pitch-based carbon fiber from BP/Amoco (recently purchased by Cytec, Greenville, TX). Eleven nylon 6,6 based formulations were produced and tested that

Correspondence to: J. A. King (jaking@mtu.edu).
Contract grant sponsor: National Science Foundation; contract grant number: DMI-9973278.
Contract grant sponsor: U.S. Department of Education; contract grant number: P200A030192.

TABLE I
Single-Filler Loading Levels

Filler	Filler concentrations
Thermocarb TC-300 specialty graphite	wt %: 10.0, 15.0, 20.0, 30.0, 40.0 vol %: 5.4, 8.2, 11.3, 17.9, 25.3
ThermalGraph DKD X	wt %: 5.0, 10.0, 15.0, 20.0, 30.0, 40.0 vol %: 2.7, 5.6, 8.6, 11.7, 18.5, 26.1

contained various amounts of these carbon fillers. There were two goals for this project. The first goal was to compare the through-plane thermal conductivity results from the guarded-heat-flow method and the transient-plane-source method. The second goal was to compare the unsteady-state thermal response of a carbon-filled composite as measured by the transient-plane-source method with a detailed finite-element analysis of heat transfer within the composite sample.

EXPERIMENTAL

Materials

The matrix used was Zytel 101 NC010 (DuPont, Wilmington, DE), an unmodified semicrystalline nylon 6,6 polymer. The fillers used were a pitch-based milled (200-μm-long) carbon fiber, ThermalGraph DKD X, from BP/Amoco (now Cytec) and Thermocarb TC-300 specialty graphite, a milled high-quality synthetic graphite available from Asbury Carbon. The properties of these polymer and carbon fillers are discussed elsewhere.[16–19]

The thermal conductivity was measured for composites containing various amounts of carbon in nylon 6,6. The concentrations (shown as weight percentages and corresponding volume percentages) for these single-filler composites are shown in Table I.

Test specimen fabrication

For this entire project, the fillers were used as received. Zytel 101 NC010 was dried in an indirectly heated, dehumidifying drying oven and then stored in moisture-barrier bags.

The extruder used was an American Leistritz Extruder Corp. model ZSE 27 extruder (Somerville, NJ). This extruder had a 27-mm, corotating, intermeshing twin screw with 10 zones and a length/diameter ratio of 40. The screw design was chosen to obtain the maximum possible conductivity and is described in detail elsewhere.[20] Hence, a minimum amount of filler degradation was desired, with the good dispersion of the fillers in the polymer maintained. The Zytel polymer pellets were introduced in zone 1. A side stuffer was located at zone 5 and was used to introduce the synthetic graphite particles into the polymer melt. Another side stuffer was located at zone 7 and was used to introduce the carbon fiber into the polymer melt. Three Schenck AccuRate gravimetric feeders (Whitewater, WI) were used to accurately control the amount of each material added to the extruder.

After passing through the extruder, the polymer strands (3 mm in diameter) entered a water bath and then a pelletizer that produced nominally 3-mm-long pellets. After compounding, the pelletized composite resin was dried again and then stored in moisture-barrier bags before injection molding.

A Niigata model NE85UA$_4$ injection-molding machine (Tokyo, Japan) was used to produce test specimens. This machine had a 40-mm-diameter single screw with a length/diameter ratio of 18. The lengths of the feed, compression, and metering sections of the single screw were 396, 180, and 144 mm, respectively.

A four-cavity mold was used to produce 63.5-mm-diameter disks (3.18 mm thick), which were the thermal conductivity test specimens. The thermal conductivity of all the formulations was determined.

Through-plane thermal conductivity test method

The through-plane thermal conductivity of a 3.18-mm-thick, 5-cm-diameter, disc-shaped test specimen was measured at 55°C with a Holometrix model TCA-300 thermal conductivity analyzer (Bedford, MA), which uses the ASTM F 433 guarded-heat-flow method.[21] The nylon 6,6 based samples were all tested dry as molded. For each formulation, at least four samples were tested.

Transient-plane-source thermal conductivity test method

A Mathis Instruments hot-disk thermal constant analyzer (Piscataway, NJ), a new instrument, was used to measure the in-plane and through-plane thermal conductivity with the transient-plane-source technique. For this test method, a nickel heating element was wound in a double-spiral pattern (diameter = 7 mm) and enclosed between two thin, electrically insulating Kapton sheets to form a sensor. The sensor was placed between two 63.5-mm-diameter composite disks to be tested. The sensor was then heated by a constant electrical current over a short period of time (typically 7 s). The generated heat dissipated within the double spiral was conducted through the Kapton insulating layer and into the surrounding sample, causing a rise in the temperature of the sensor and the sample. The average transient temperature increase of the sensor was simultaneously measured by the recording of the change in the electrical resistance,[22–24] from which the through-plane and in-plane thermal conductivities were obtained. The nylon 6,6 based samples were all tested dry as molded and at 23°C. For each formula-

TABLE II
Comparison of Thermal Conductivity Results[26]

Formulation (wt %)	TCA 300 through-plane thermal conductivity (W/m K)	Hot-disk through-plane thermal conductivity (W/m K)	Hot-disk in-plane thermal conductivity (W/m K)
Synthetic graphite particles			
10	0.386 ± 0.008, $n = 4$	0.391 ± 0.015, $n = 5$	1.701 ± 0.092, $n = 5$
15	0.466 ± 0.023, $n = 4$	0.483 ± 0.022, $n = 5$	1.792 ± 0.028, $n = 5$
20	0.566 ± 0.044, $n = 5$	0.599 ± 0.013, $n = 5$	2.563 ± 0.120, $n = 5$
30	0.819 ± 0.056, $n = 12$	0.956 ± 0.040, $n = 10$	3.179 ± 0.117, $n = 10$
40	1.077 ± 0.103, $n = 7$	1.219 ± 0.057, $n = 5$	4.949 ± 0.114, $n = 5$
Carbon fiber			
5	0.327 ± 0.002, $n = 4$	0.302 ± 0.025, $n = 5$	2.309 ± 0.257, $n = 5$
10	0.349 ± 0.013, $n = 5$	0.333 ± 0.036, $n = 5$	2.557 ± 0.086, $n = 5$
15	0.387 ± 0.006, $n = 4$	0.369 ± 0.016, $n = 5$	3.639 ± 0.125, $n = 5$
20	0.481 ± 0.020, $n = 8$	0.447 ± 0.015, $n = 10$	4.352 ± 0.133, $n = 10$
30	0.675 ± 0.043, $n = 4$	0.679 ± 0.013, $n = 5$	5.039 ± 0.236, $n = 5$
40	0.950 ± 0.106, $n = 6$	1.034 ± 0.046, $n = 5$	6.733 ± 0.126, $n = 5$

tion, five different sets (one set of two disks with the sensor between them) of samples were tested. The results are listed in Table II and are described later.

Filler length and aspect ratio test method

To determine the length of the carbon fiber and synthetic graphite in the test specimens, solvent digestion was used. A 0.2-g sample cut from the center of a thermal conductivity specimen was dissolved at 23°C with formic acid to remove the nylon 6,6. The fillers were then dispersed onto a glass slide and viewed with an Olympus SZH10 optical microscope (Melville, NY) with an Optronics Engineering LX-750 video camera (Goleta, CA). The images (at a magnification of 60×) were collected with Scion Image software (version 1.62). The images were then processed with Adobe Photoshop (version 5.0) and the Image Processing Tool Kit (version 3.0). The length and aspect ratio (length/diameter) of each filler were measured. For each formulation, 1000–6000 particles/fibers were measured.[25–27]

Filler orientation test method

To determine the orientation of the carbon fillers, a polished composite sample was viewed with an optical microscope. One square (13 mm × 13 mm) was cut from the center of each through-plane thermal conductivity sample. These samples were cast in two-part epoxy plugs so that the 3.18-mm face (through the sample thickness) could be viewed. The samples were then polished and viewed with an Olympus BX60 reflected light microscope at a magnification of 200×. Again, the images were collected with Scion Image software (version 1.62). The images were then processed with Adobe Photoshop (version 5.0) and the Image Processing Tool Kit (version 3.0). For each formulation, the orientation was typically determined by the viewing of 1000–6000 particles/fibers. Additional test method details are discussed elsewhere.[26–28]

RESULTS

Filler length and aspect ratio results

The length and aspect ratio of the as-received synthetic graphite particles (Thermocarb TC-300 specialty graphite) were 68.3 μm and 1.80, respectively. The length and aspect ratio of the synthetic graphite particles in the composite specimens were typically 62–70 μm, and 1.67–1.69, respectively.[20,25–29] Hence, the length and aspect ratio of the synthetic graphite particles in the composite specimens remained similar to those of the as-received material. This result was likely due to the relatively small length and aspect ratio of the as-received Thermocarb TC-300 specialty graphite.

Before processing, the mean length of the carbon fibers was 167.5 μm with an aspect ratio (length/diameter) of 16.75. This compared well with the reported vendor literature value of a 200-μm mean carbon fiber length.[17] For all the carbon fiber/nylon 6,6 composites, the length varied from 90 to 100 μm, and the aspect ratio varied from 9 to 10. For example, in the 20 wt % carbon fiber/nylon 6,6 composites, the length and aspect ratio of the carbon fiber were 97 μm and 9.7, respectively.[20,25–29] Overall, processing reduced the carbon fiber length and aspect ratio to approximately half of the as-received values. These length results were comparable to those reported by Bigg,[30] who showed that carbon fiber/nylon 6,6 composites had fiber lengths of approximately 130 μm after extrusion and injection molding.

Filler orientation results

As discussed previously, the filler orientation angle was measured by optical microscopy. All the angles were between 0 and 90°. An angle of 0° signified that the fibers were aligned parallel to the thermal conductivity measurement direction. An angle of 90° meant that the fibers were perpendicular to the thermal conductivity measurement direction.

The mean orientation angle varied from 58 to 62° for all the composites containing Thermocarb TC-300 specialty graphite.[20,25–28] For the sample containing 30 wt % Thermocarb TC-300 specialty graphite, the mean orientation angle was 58° with a standard deviation of 25° (3784 particles measured). A photomicrograph of a composite containing this filler is shown elsewhere.[31] The orientation angle was closer to 90°, and this indicated that the particles were primarily oriented transversely to the through-plane thermal conductivity measurement direction.

For all the carbon fiber/nylon 6,6 composites, the mean orientation angles varied from 63 to 72°.[20,25–28] A photomicrograph of a composite containing this filler is shown elsewhere.[19] Hence, the orientation angle was closer to 90°, and this indicated that the fibers were primarily oriented transversely to the through-plane thermal conductivity measurement direction.

Thermal conductivity results

Table II displays the mean standard deviation and number of samples tested for the through-plane thermal conductivity with the TCA 300 (guarded-heat-flow method) and the hot disk (transient-plane-source method), as well as the in-plane thermal conductivity as measured by the hot disk. The thermal conductivity of the neat polymer was 0.25 W/m K.[16] The results in Table II indicate that the through-plane thermal conductivity was similar for both test methods. For example, for the composite containing 30 wt % carbon fiber in nylon 6,6, the through-plane thermal conductivity was 0.675 ± 0.043 W/m K, as measured by the guarded-heat-flow method, in comparison with 0.679 ± 0.013 W/m K, as measured by the transient-plane-source method. As expected, the in-plane thermal conductivity was higher than the through-plane thermal conductivity. For the composites containing synthetic graphite particles, the in-plane thermal conductivity was typically 4 times larger than the through-plane thermal conductivity. For the composites containing carbon fibers, the in-plane thermal conductivity was typically 7 times larger than the through-plane thermal conductivity. The higher in-plane thermal conductivity for the composites containing carbon fibers was likely due to the higher aspect ratio of the carbon fibers (typically 9.7) in comparison with the synthetic graphite (typically 1.7).

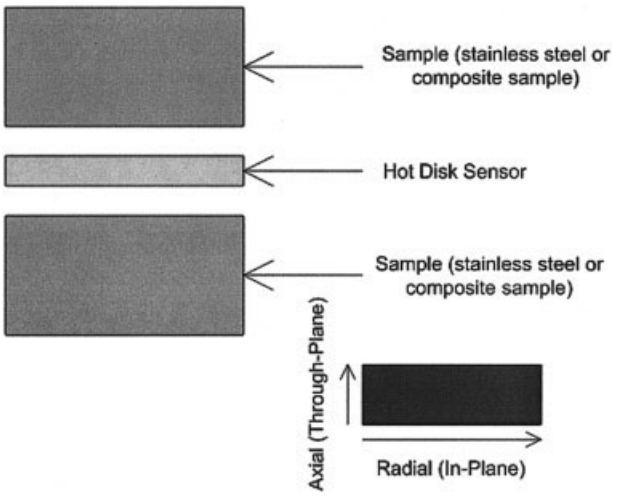

Figure 1 Schematic of the samples and sensor.

MODELING BACKGROUND AND RESULTS

The primary purpose for creating a finite-element model of the hot disk was to obtain a better conceptual understanding of the equipment and of the data analysis software that it uses. The model also has potential future material design applications.

Hot-disk apparatus

The hot-disk apparatus is composed of the following pieces of equipment:

- A double-spiral sensor composed of a thin nickel film that is embedded in a thin layer of Kapton. A given quantity of power is dissipated through this spiral for a given amount of time. The temperature rise of the sensor is calculated by the measurement of the resistance of the nickel, which is a well-defined function of temperature. The change in temperature as a function of time is calculated by the following formula:

$$\Delta T(t) = \left[\frac{1}{\alpha}\left(\frac{R(t)}{R_0} - 1\right)\right] \quad (1)$$

where $\Delta T(t)$ is the change in temperature at time t (K), α is the temperature coefficient of resistance of the material (1/K), $R(T)$ is the electrical resistance of the nickel at time t (Ω), and R_0 is the electrical resistance of the nickel at time 0 (Ω).

A minimum of two sample disks, one of which is placed underneath the sensor in direct contact with it and one of which is placed above the sensor in direct contact with it. The sensor is placed at the center of the sample disks. Figure 1 illustrates this setup.

A metal bar suspended over the sample with a small screw in the center. This screw provides pressure on a

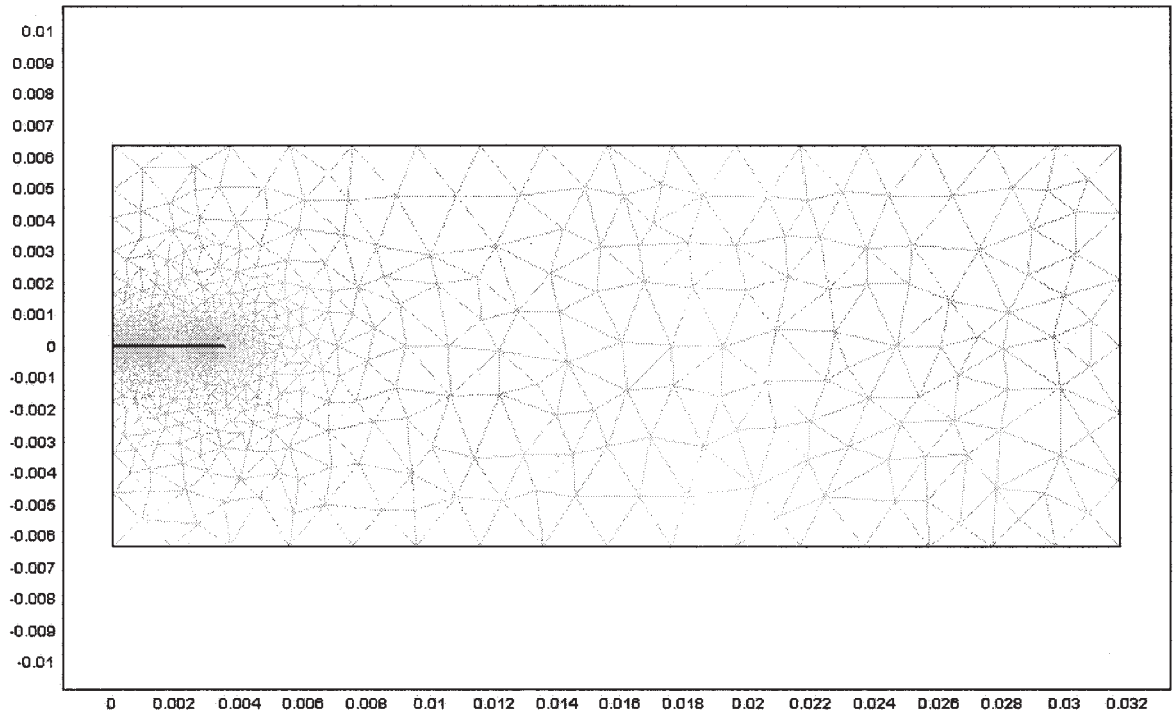

Figure 2 FEMLAB mesh for composite sample analysis (the units are meters for both axes).

small steel plate, which is set on top of the sample stack. This pressure is adjusted to ensure firm contact between the sensor and the sample.

A cylindrical shell cover that goes over the top of all of the above to minimize temperature- and air-movement variations during and between experiments.

FEMLAB

The FEMLAB modeling program[32] (version 3.0) uses the finite-element method to solve problems in transport phenomena. Using the standard heat-transfer equations, the known physical properties of the materials, and a given time step and time range, FEMLAB then proceeds to solve for the temperature distribution throughout the sample. Depending on the degree of accuracy that is desired, the number of elements can be increased. This increase can be localized to a small portion of the geometry or applied to the entire geometry, as desired. The relevant heat-transfer equation that FEMLAB solves is

$$\rho C_p \frac{\partial T}{\partial t} - \nabla(k\nabla T) = Q \qquad (2)$$

where ρ is the density of the sample (kg/m^3), C_p is the heat capacity of the sample [J/(kg K)], T is the temperature of the sample (K), t is the time of the measurement (s), k is the thermal conductivity of the sample (W/m K), and Q is the power supplied to the sensor per unit of volume (W/m^3). The sample is assumed to be symmetric about the center vertical axis (θ symmetry in cylindrical coordinates). Figure 2 shows an image of the mesh generated by FEMLAB for the composite sample analysis. This mesh was the original mesh suggested by FEMLAB and contained 4734 elements; any increase in the number of elements had an insignificant impact on the system solution. A similar mesh was used in the stainless steel standard analysis. In Figure 2, the thick, black line that starts at (0,0) and extends into the larger rectangle is the sensor; the larger rectangle is the sample. The boundary conditions imposed on the system were as follows: a continuity of temperature and flux existed at the interface between the sample and the sensor and at the left boundary (which is the center of the sample disks); all other boundaries were presumed to be no-flux boundaries.

Generation of the FEMLAB model: stainless steel standard

The standard used in the calibration of the hot disk was a pair of 50-mm-diameter, 20-mm-thick stainless steel cylinders [American Iron and Steel Institute 316]. One 20-mm-thick stainless steel sample was placed above the sensor. The other 20-mm-thick stainless steel sample was placed below the sensor. In FEMLAB, the change in temperature was measured as a deviation from room temperature with the following formula:

TABLE III
Physical Properties of Stainless Steel Standard and Sensor[22]

Property (units), nomenclature	Stainless steel standard	Hot-disk sensor
Radius (mm), (r)	25	3.5
Thickness (mm), (h)	20	0.02
Thermal conductivity (W/mK), (k)	14.85	91
Density (kg/m^3), (ρ)	8000	8900
Heat capacity [J/(kg K)], (C_p)	500	520
Heat source (W/m^3), (Q)	0	1.3×10^9

$$\Delta T = T_{\text{sensor}}(t) - T_{\text{room}}(t) \quad (3)$$

where ΔT is the change in temperature (K), $T_{\text{sensor}}(t)$ is the temperature at the center of the sensor at time t (K), and $T_{\text{room}}(t)$ is the temperature of the room at time t (K). To directly measure the temperature rise, $T_{\text{room}}(t)$ was standardized to 0 K. The sensor was treated as a thin disk of metal with a uniform heat source. Furthermore, because the sensor thickness (0.02 mm) was very small with respect to the sample thickness (20 mm), the system was treated as having the sample disks in direct and perfect contact at all x-axis (radial) coordinates greater than the radius of the sensor. The physical properties of the stainless steel standard and the sensor are given in Table III.[22]

FEMLAB was used to solve this system over the time interval $t = 0$ to 5 s with data output at intervals of 0.025 s. The simulation data were compared to the experimental data generated by the hot disk. The same set of stainless steel samples were tested eight times. Power (1.00 W) was supplied to the sensor for 5 s. In the hot disk, the temperature rise was calculated at the center of the sensor. FEMLAB predicted the unsteady-state temperature response of the solid; this response was plotted versus time at the center of the sensor. The experimental data were analyzed in the following manner:

- The data were averaged at each time step.
- The data were standardized. This standardization consisted of subtracting the average temperature at $t = 0.025$ s from itself and each subsequent average temperature. This data set is titled "Average Temperature" on the figures that follow. The data were standardized because the data from the first time interval were collected before the sensor was in the steady state and were not indicative of the performance of the system.
- The standard deviation of the data values at each time step was calculated with the 8 data sets collected.
- The standard deviation at each time step was added to the average temperature of the same time step. This data set is titled "+1 Standard Deviation" on the figures that follow.
- The standard deviation at each time step was subtracted from the average temperature of the same time step. This data set is titled "−1 Standard Deviation" on the figures that follow.

These three data sets were plotted against the FEMLAB results. The FEMLAB data set is labeled "FEMLAB" on the figures that follow. Figure 3 shows a comparison between the hot disk and FEMLAB for the stainless steel standard. After 5 s, the hot disk measured a temperature rise of 2.43 K at the center of the sensor; the FEMLAB result predicted a temperature rise of 2.48 K. As the figure shows, the FEMLAB data show a good fit with the hot-disk data, with a small undershoot at the beginning and a very small overshoot at the end.

Generation of the FEMLAB model: composite samples

To determine the through-plane (axial) and in-plane (radial) thermal conductivities, four 63.5-mm-diameter, 3.18-mm-thick composite samples of the same formulation were used with the hot disk: two composite samples above the sensor and two composite samples below the sensor. For each formulation, the same set of four composite samples was tested 10 times. Power (0.05 W) was supplied to the sensor for 5 s. With FEMLAB, the change in temperature at the center of the sensor was calculated, as described in the previous subsection, with the physical properties of the composite samples and the sensor given in Table IV.[22]

Figure 4 shows a comparison between the hot disk and FEMLAB for the composite containing 30 wt % synthetic graphite. After 5 s, the hot disk measured a temperature rise of 0.87 K at the center of the sensor;

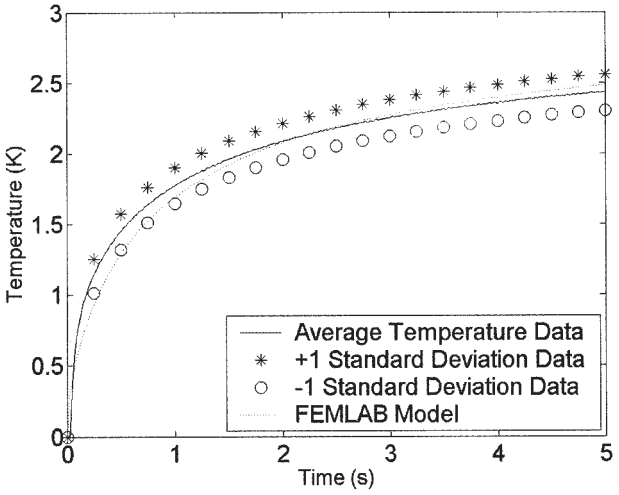

Figure 3 Stainless steel standard: hot disk versus FEMLAB.

TABLE IV
Physical Properties of Representative Composites and Sensor[22]

Property (units), nomenclature	30 wt % synthetic graphite particles	20 wt % carbon fiber	Hot-disk sensor
Radius (mm), (r)	31.75	31.75	3.5
Thickness (mm), (h)	6.36	6.36	0.02
Density (kg/m^3), (ρ)	1340	1260	8900
Heat capacity [J/(kg K)], (C_p)	840	870	520
Heat source (W/m^3), (Q)	0	0	6.5e7

the FEMLAB result predicted a temperature rise of 0.86 K at the same point. Figure 5 shows a comparison between the hot disk and FEMLAB for the composite containing 20 wt % carbon fiber. After 5 s, the hot disk measured a temperature rise of 1.18 K at the center of the sensor; the FEMLAB result predicted a temperature rise of 1.15 K at the same point. The trends were the same as that seen in the stainless steel standard test.

CONCLUSIONS

The first goal of this work was to compare the through-plane thermal conductivity results from the guarded-heat-flow method and with the transient-plane-source method. The results of this study show that both test methods give similar values for through-plane thermal conductivity. The advantage of the transient-plane-source method is that it provides both the through-plane and in-plane thermal conductivities. The experiment also takes less time than the guarded-heat-flow method. The disadvantage of the transient-plane-source method is that additional material properties (density and heat capacity) of the anisotropic composite material are required to determine the thermal conductivity.

The second goal of this work was to compare the unsteady-state thermal response of a carbon-filled composite as measured by the transient-plane-source method with a detailed finite-element analysis of heat transfer within the composite sample. The results indicate that the finite-element model is useful in accurately predicting the thermal response of the composite material. The model can be used in future design applications.

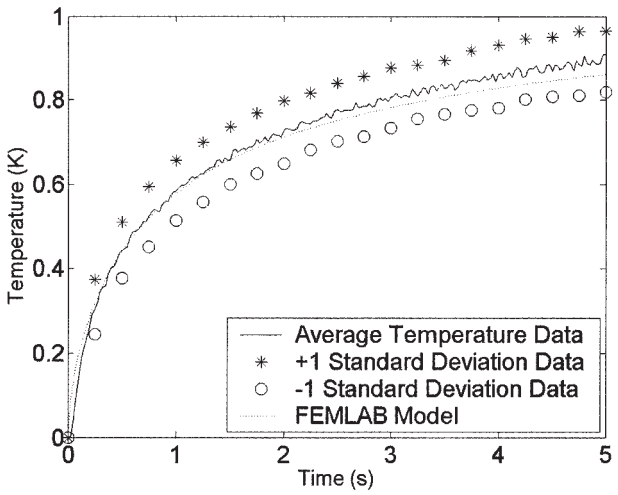

Figure 4 Synthetic graphite (30 wt %) in nylon: hot disk versus FEMLAB.

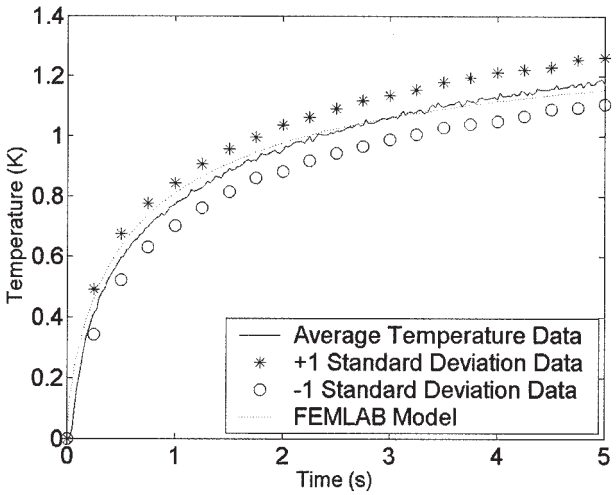

Figure 5 Carbon fiber (20 wt %) in nylon: hot disk versus FEMLAB.

References

1. Finan, J. M. Proc Soc Plast Eng Annu Tech Conf 1999, 1547.
2. Agari, Y.; Uno, T. J. J Appl Polym Sci 1985, 30, 2225.
3. Bigg, D. M. Polym Eng Sci 1977, 17, 842.
4. Bigg, D. M. Adv Polym Technol 1984, 4, 255.
5. Narkis, M.; Lidor, G.; Vaxman, A.; Zuri, L. J Electrost 1999, 47, 201.
6. Nagata, K.; Iwabuki, H.; Nigo, H. Compos Interfaces 1999, 6, 483.
7. Demain, A. Ph.D. Dissertation, Universite Catholique de Louvain, 1994.
8. King, J. A.; Tucker, K. W.; Meyers, J. D.; Weber, E. H.; Clingerman, M. L.; Ambrosius, K. R. Polym Compos 2001, 22, 142.
9. Murthy, M. V. Proc Soc Plast Eng Annu Tech Conf 1994, 1396.
10. Simon, R. M. Polym News 1985, 11, 102.
11. Mapleston, P. Mod Plast 1992, 69, 80.
12. Bigg, D. M. Polym Compos 1986, 7, 125.
13. Issi, J.-P.; Nysten, B. In Carbon Fibers, 3rd ed.; Donnet, J. B.; Rebouillat, S.; Wang, T. K.; Peng, J. C. M., Eds.; Marcel Dekker: New York, 1998; Chapter 6.
14. Brosius, B. High Performance Compos 2001, 5, 22.
15. Thongruang, W.; Spontak, R. J.; Balik, C. M. Polymer 2002, 43, 3717.

16. DuPont Zytel Nylon Resin Product and Properties, Version 95.9; DuPont Engineering Polymers: Wilmington, DE, 1995.
17. BP/Amoco Performance Products: High Thermal Conductivity Pitch Based Graphite Fibers; Amoco Polymers: Alpharetta, GA, 1996.
18. Conoco Carbon Products Product Literature; Conoco: Houston, TX, 1999.
19. Clingerman, M. L.; Weber, E. H.; King, J. A.; Schulz, K. H. Polym Compos 2002, 23, 911.
20. Krueger, Q.; King, J. A. Adv Polym Technol 2003, 22, 96.
21. Evaluating Thermal Conductivity of Gasket Materials; ASTM Standard F 433-77; American Society for Testing and Materials: Philadelphia, 1996.
22. Hot Disk Thermal Constants Analyser Instruction Manual; Mathis Instruments: Fredericton, Canada, 2001.
23. Gustavsson, M.; Karawacki, E.; Gustafsson, S. E. Rev Sci Instrum 1994, 65, 3856.
24. Log, T.; Gustafsson, S. E. Fire Mater 1995, 19, 43.
25. Clingerman, M. L. Ph.D. Dissertation, Michigan Technological University, 2001.
26. Weber, E. H. Ph.D. Dissertation, Michigan Technological University, 2001.
27. Konell, J. P. Ph.D. Dissertation, Michigan Technological University, 2002.
28. Heiser, J. A.; King, J. A. Polym Compos 2004, 25, 186.
29. Konell, J. P.; King, J. A.; Miskioglu, I. J Appl Polym Sci 2003, 90, 1716.
30. Bigg, D. M. Polym Compos 1985, 6, 20.
31. Weber, E. H.; Clingerman, M. L.; King, J. A. J Appl Polym Sci 2003, 88, 112.
32. FEMLAB 3.0 Manual; COMSOL: Burlington, MA, 2004.